Savunma Bilimleri Dergisi, 43(2): 454-472 (2023)

Elektronik/Online ISSN: **2148-1776**

Basılı/Printed ISSN: **1303-6831**

https://dergipark.org.tr/tr/pub/khosbd

SAVUNMA BİLİMLERİ DERGİSİ

The Journal of Defense Sciences

Aluminum and Carbon Fiber Reinforced Polymer Composite Material Comparative Strength Analysis of a Structural Part in F-16 Fighter Aircraft Landing Gear

F-16 Savaş Uçağı İniş Takımındaki Yapısal Bir Parçanın Alüminyum ve Karbon Fiber Takviyeli Polimer Kompozit Malzeme Karşılaştırmalı Mukavemet Analizi

İlteriş KAYA [1] Mehmet ÇEVİK [2,*]

[1]*Türk Hava Kuvvetleri, Savunma Plan Proje Yönetim Başkanlığı, 06100, Çankaya/ANKARA*

[2]*İzmir Kâtip Çelebi Üniversitesi, Mühendislik ve Mimarlık Fakültesi, Makina Mühendisliği Bölümü, 35620, Çiğli /İZMİR*

Makale Bilgisi

Araştırma makalesi
Başvuru: 28.01.2023
Düzeltme: 22.02.2023
Kabul: 27.02.2023

Keywords

F-16 fighter aircraft
Weight reduction
Carbon fiber reinforced polymer (CFRP) composite material
Finite element method (FEM)

Anahtar Kelimeler

F-16 savaş uçağı
Ağırlık azaltma
Karbon fiber takviyeli polimer kompozit malzeme
Sonlu elemanlar metodu (SEM)

Abstract

In this study, the geometric structure, weight and boundary conditions of the aluminum alloy main landing gear FS 34.180 structural part currently used in F-16 fighter aircraft are determined. Finite element (FE) analysis is performed considering the forces that the existing part is exposed to in four different scenarios with Ansys Workbench software. Then, a FE model of the same part is created from carbon fiber reinforced polymer (CFRP) composite material. The loading conditions applied in the four scenarios are also applied to the new CFRP composite material model. Equivalent stress, equivalent total strain, maximum shear stress and total deformation values in the models created with both materials are calculated. The results obtained for both materials are compared. As a result of the comparison, it is observed that there is a decrease of approximately 0.8% in the equivalent stress, 12% in the equivalent total strain, 0.7% in the maximum shear stress and 11.8% in the total deformation values for the same loading and boundary conditions. In addition, the total mass of the part is reduced from 31.17 kg to 20.77 kg, which corresponds to a reduction of 33.37%. This development is expected to reduce the weight of the aircraft as well as extend the fatigue life and maintenance period.

Özet

Bu çalışmada, F-16 savaş uçaklarında hâlihazırda kullanılmakta olan alüminyum alaşımlı ana iniş takımı FS 341.80 kodlu yapısal parçasının geometrik yapısı, ağırlığı ve sınır şartları tespit edilmiştir. Mevcut parçanın, dört farklı senaryo durumunda maruz kaldığı kuvvetlere göre sonlu elemanlar analizi Ansys Workbench yazılımı ile yapılmıştır. Ardından, aynı parçanın karbon fiber takviyeli polimer kompozit malzemeden sonlu eleman modeli oluşturulmuştur. Önceki dört senaryoda uygulanan yükleme durumları yeni kompozit malzeme modele de uygulanmıştır. Her iki malzeme ile oluşturulmuş modellerdeki eşdeğer gerilme, eşdeğer toplam gerinim, maksimum kayma gerilmesi ve toplam deformasyon değerleri hesaplanmıştır. Her iki malzeme için elde edilen sonuçlar karşılaştırılmıştır. Karşılaştırma sonucunda aynı yükleme ve sınır şartları için eşdeğer gerilme değerlerinde yaklaşık %0.8, eşdeğer toplam gerinim değerlerinde yaklaşık %12, maksimum kayma gerilmesi değerlerinde yaklaşık %0.7 ve toplam deformasyon değerlerinde yaklaşık %11.8 civarında azalma olduğu görülmüştür. Bunun yanında parçanın toplam kütlesi 31.17 kg'dan 20.77 kg'a inmiş; yani, %33,37 oranında azalma sağlanmıştır. Bu gelişmenin, uçağın ağırlığını azaltmanın yanında yorulma ömrünü ve bakım süresini de uzatması beklenmektedir.

*Mehmet ÇEVİK, e-mail: mehmet.cevik@ikcu.edu.tr

DOI: 10.17134/khosbd.1243616

1. INTRODUCTION

The practice of composite materials is steadily broadening in the aerospace industry as well as in many areas. Especially polymer composite materials have a leading and essential effect on the aviation industry. Today, approximately 30-40 percent of aircraft frames are manufactured using composite materials and this rate is escalating constantly due to technological developments in this field. Especially, fiber-reinforced polymer composite materials are rapidly proliferating in the production of aircraft and space vehicles (Megson, 2018).

Engineering materials fall into several categories: metals, polymers, ceramics and inorganic glasses, and composites. Metals perform very good at medium temperatures but are not as favorable as ceramics at high temperatures. On the other hand, ceramics have high brittleness which makes them inefficient in many cases. Polymeric materials usually fail in medium to high temperatures. Therefore all of them have pros and cons.

Polymer composites are highly efficient, environmentally friendly and provide significant weight reduction. Because of the high strength of their fibers, polymer composites offer high "strength-to-weight" and "hardness-to-weight" ratios (Adeniran et al., 2022; Faizan & Gangwar, 2021; Savran et al., 2022; Kandaş & Özdemir, 2022). Apart from that, they have high shear strength and low density. For these reasons, new generation of aerospace engineers prefer polymer composites to make aircraft lighter, stronger and more fuel efficient.

The performance of aircrafts are greatly affected by their weight since overloading causes severe problems. Using composite materials contributes to the solution of this problem. As the aircraft operates in a very corrosive environment, corrosion damage must be considered. Non-corrosive carbon fiber and glass fiber reinforced polymers were first used in aircraft in the 1970s. Since those years, the use of composite materials has been increasing rapidly (Atique et al., 2014; Nayak, 2014; Mrazova, 2013; Deo et al., 2003).

F-16 aircrafts are used in the airforces of many countires. Manufactured by General Dynamics and Lockheed Martin companies, these aircraft have various models for training, fighting and bombing purposes (Han et al., 2009). F-16 aircraft has a total length of 15 m, a wingspan of about 10 m, a height of 5 m, a curb weight of about 8280 kg, and a maximum speed of Mach 2.05, with a single engine capable of providing 102 to 130 kilonewtons of thrust. Aluminum constitutes approximately 83% of the material in the fuselage and landing gear of these aircraft; steel, titanium and various other materials are also used (Crosby, 2015).

In this study, an alternative for the production of the aluminum alloy FS 341.80 structural part in the lower section of the main landing gear used in F-16 aircraft with CFRP composite material was discussed and the comparative aluminum alloy and CFRP composite material strength analysis was performed using Ansys Workbench FE software.

2. MATERIALS USED IN THE STUDY

2.1 Carbon Fiber Reinforced Polymer (CFRP) Composite Material

A composite material is a multiphase structural material made of two or more materials with substantially distinctive physical or chemical properties, which when blended offer superior overall performance compared to individual components. Composites usually consist of two components; the reinforcement which consists of stronger, rigid and load-bearing components embedded in a weaker, less rigid matrix. The reinforcements are usually fibers or particles. The matrix is a polymer, metal, cement, ceramic or hybrid material.

Composite materials are classified in various ways. According to the matrix materials, they are classified as metal matrix, ceramic matrix and polymer matrix composites. According to the fiber type, they are classified as particle-reinforced, fiber-reinforced and structural composites. Composite materials, although slightly more expensive, have gained more popularity as high-performance products that need to be light in weight but strong enough to carry heavy loads. Aircraft and spacecraft structures, boat and ship hulls, bicycle and race car body frames, wind turbine blades, etc. are some of them. (Mangalgiri, 1999; Atique et al., 2014; Guo, et al., 2022; Jung, et al., 2022; Karslı et al., 2020)

In this study, the production of a structural part used in F-16 aircraft from CFRP composite material as an alternative for aluminum alloy is discussed for the aim of weight reduction. For this purpose, a 3D model was first created with Unigraphics NX 7.5 CAD software based on technical drawings developed on an existing part and then imported into Ansys Workbench FE software to perform equivalent static analysis. The mechanical properties of the CFRP composite used as an alternative in the analysis are given in Table 1.

Table 1: Mechanical Properties of the Materials Used

Mechanical Property	Aluminum alloy (Al 2024-T351)	CFRP composite material
Yield stress, σ_y [MPa]	241.32	400.00
Ultimate stress, σ_{UTS} [MPa]	351.63	450.00
Modulus of elasticity, E [GPa]	73.77	395.00
Shear modulus, G [GPa]	27.58	141.07
Poisson's ratio, ν	0.33	0.40

2.2 Aluminum Alloy Material

The part currently used in the F-16 is made of an aluminum and copper alloy called Al 2024-T351. Aluminum alloys are extensively used in the aerospace industry (Starke & Staley, 1996; Özer, 2016). The Aerospace Materials Specification (AMS) assigns the code AMS-QQ-A-250/5 to this alloy, a wide-known one. T351 means that the alloy has undergone a final high temperature heat treatment. Its main properties are high ductility, high creep resistance at elevated temperatures and high fracture toughness (Gökçe, 2021; Mouritz, 2012; Özer et al., 2022; Altuntaş & Bostan, 2022; Pan et al., 2023). The

mechanical properties of this material are also given in Table 1 comparatively (Holt et al., 1997; MMPDS handbook, 2023).

3. METHOD OF THE STUDY

3.1 Finite Element Method (FEM)

In this study, FEM –a widely used numerical method in engineering analysis and designs– was employed. In physical systems with complex geometries, loadings, and material properties, it is often not possible to obtain analytical solutions to simulate the system's response. Analytical solutions are given by a mathematical expression that gives the values of unknown quantities desired in any part of an object and is therefore valid for an infinite number of positions in the body. These solutions often require solving ordinary or partial differential equations created by engineers and mathematicians. Because of the complex geometries, loadings and material properties, the solution of these differential equations is not easily obtained. For this reason, numerical methods such as FEM are used (Müftü, 2022; Stolarski et al., 2018; Logan, 2016; Cevik, 2009).

In FE stress analysis, the real geometric body is formed from elements that are easy to calculate on the computer, due to the difficulty of formulating it exactly. The laws of physics are then applied to each of these small elements having simpler geometry. A mesh structure is developed to divide the whole body into elements. The division of the object into elements selected in accordance with its size and geometry is called meshing. Nodal points are generated where the elements come into contact with each other. It is important to use as many elements as possible so that the stress distribution can be measured more sensitively. The coordinates of all nodes are determined with respect to the origin. In the mathematical model, matrices are formed for the situations that occur with the application of external forces and boundary conditions to the nodes, and these matrix equations are solved by software. In this way, the stresses and strains in each element and therefore in the entire body formed by the elements are obtained. In the application of the FEM to elastic and continuous media, the steps are: dividing the structure into parts, choosing an appropriate interpolation function, deriving the global equilibrium equations by combining the element stiffness matrices, applying load and boundary conditions, solving the global equation and determining the nodal displacements, strains, stresses and other unknown results (Logan, 2016; Stolarski et al., 2018) The information required in order to solve these problems are: (a) the geometric model of the body, (b) the mechanical properties of the elements such as modulus of elasticity, (c) initial, boundary and loading conditions, (d) type of analysis to be performed.

3.2 The FE Software Used in the Analysis

Ansys Workbench software was used for FE analysis. It is a general purpose FE software that can be used to simulate the interaction of all engineering disciplines in the fields of strength, vibration, fluid mechanics, heat transfer, and electromagnetics. Its reliability has been accepted all over the world with its widespread use for many years (Esen & Ülker, 2005; Stolarski et al., 2018; Tunca & Kafalı, 2021;

Godara et al., 2022; Sunar & Cevik, 2015; Silori et al., 2015; Hassan & Kurgan, 2019). Ansys Workbench enables the simulation of the working conditions and the tests of the products in the virtual environment before the prototypes are produced. This software graphically displays the distribution of strains, stresses and all other calculated results.

3.3 The FE Type Used in the Analysis

In the FE analysis, Ansys Workbench SOLID 186/187 element type was used. SOLID186 is a higher order 3-D solid element that features quadratic displacement behavior. It has 20 nodes and 3 degrees of freedom at each node: translations in the nodal x, y, and z directions. SOLID 187 is the pyramid version of the same element. This element supports plasticity, hyperelasticity, creep, large deflection, and large strain capabilities. (See Figure 1)

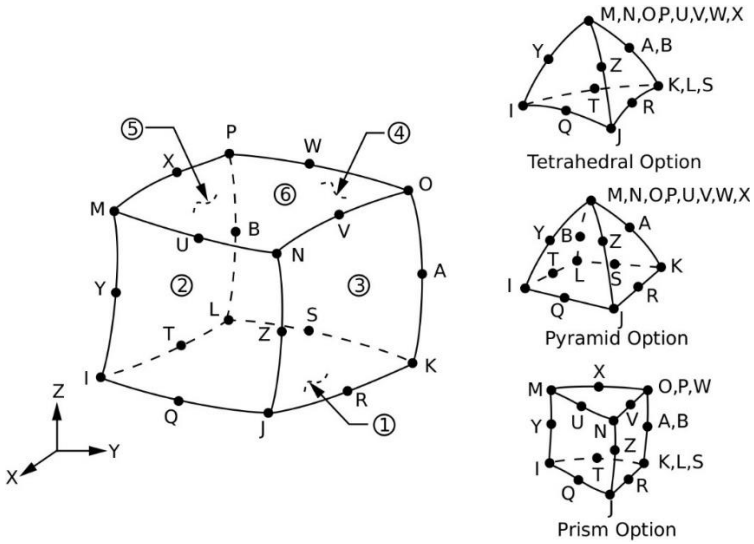

Figure 1: Solid 186/187 Element Used in Ansys Workbench
(Ansys Workbench Manual)

3.4 Convergence Analysis

In FEM, the displacement solutions converge when the solutions asymptotically tend to a certain value (Logan, 2016; Diambu & Cevik, 2022). Since more accurate results are required in the analysis, mesh convergence analysis was performed in the beginning. As the number of elements of the mesh increases, the analysis results approach those of the exact solution. This gives an idea of how small the elements should be to ensure that the FE analysis results are not affected by the change in mesh size.

3.5 Numerical Results Considered in the Analysis

For ductile materials, the most common yield criterion is the von Mises Yield Criterion, also known as the equivalent stress criterion. It states that the material will yield if the equivalent stress of a material under the loading is equal to or greater than the yield limit of the same material under simple stress (Stolarski et al., 2018). Thus, the von Mises stress is used to predict the yield of materials under complex loading conditions. The equivalent stress (σ_{eq}) is expressed in Eq. (1), which is also used in Ansys Workbench.

$$\sigma_{eq} = \sqrt{\frac{1}{2}[(\sigma_1 - \sigma_2)^2 + (\sigma_2 - \sigma_3)^2 + (\sigma_3 - \sigma_1)^2]} \quad (1)$$

In our study, apart from equivalent stress; equivalent total strain, maximum shear stress and total deformation values were also taken into account. Strain designates the deformation of a body under the effects loads such as loads and pressure, etc. Equivalent strain, as a scalar, is a straightforward variable to report strain results over a body. Shear stress is the stress component parallel to the material cross section. Total deformation exhibits all the deformation pertinent to the model, in three Cartesian coordinates.

4. DEFINING THE CRITICAL COMPONENT TO ANALYZE

4.1 Selecting the Critical part

The main landing gear is extremely important to the aircraft, especially when landing (Megson, 2018; Göker et al., 2021). The aircraft puts more effort than at any other phase during the landing phase. FS 341.80 is the component that provides the connection between the aircraft fuselage (see Figure 2) and the landing gear; thus, it is exposed to much more force during landing than most components of the aircraft.

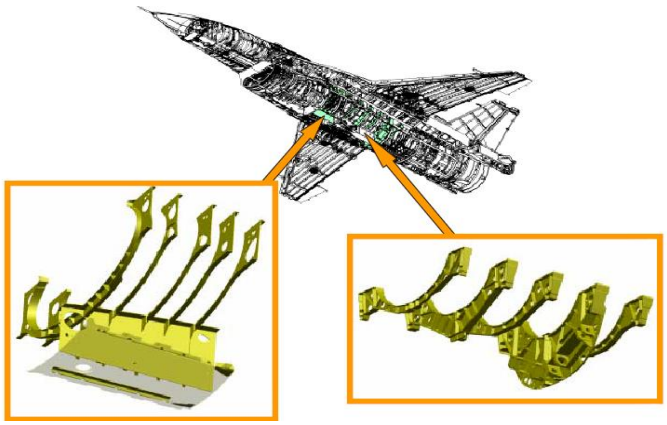

Figure 2: F-16 Aircraft Lower Fuselage Structure
(Lockheed Martin Aeronautics Company)

Figure 3: Part FS 341.80

The main landing gear shock struts and strap struts are attached to the fuselage on part FS 341.80 (See Figure 3). We decided to select this part for our study, which is located in lower side of the main landing gear.

4.2 Modeling the Part to be Analyzed

Since the original technical drawings of the manufacturer could not be accessed, dimensions were taken on an existing part. Modeling based on these dimensions was performed using Unigraphics NX 7.5 3D software, which is compatible with Ansys Workbench. This part has a very complex geometry, which contains many ribs of varying thickness and some curved surfaces. As seen in Figure 4, the modeled geometry is 1470 mm wide and 700 mm high, its thickness is 120 mm. Figure 5 shows the isometric view of the part.

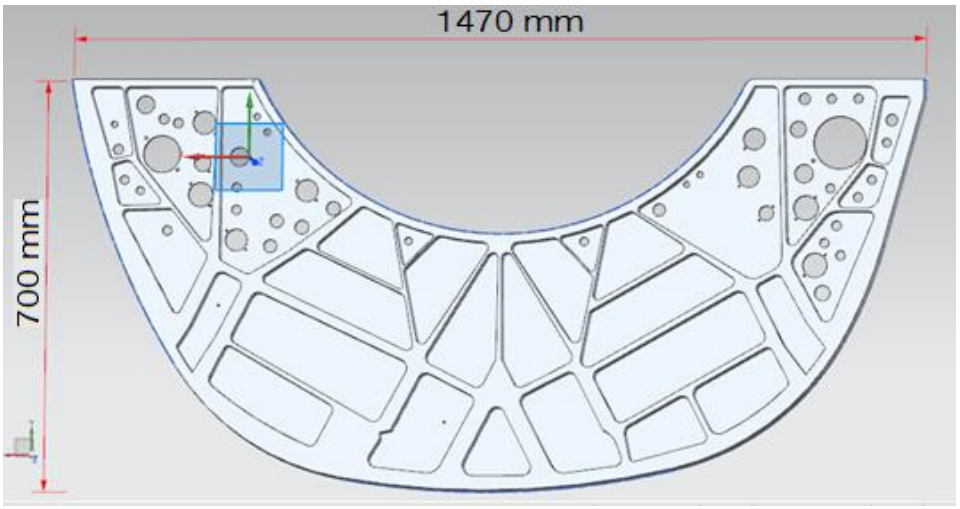

Figure 4: Front View of the Part FS 341.80

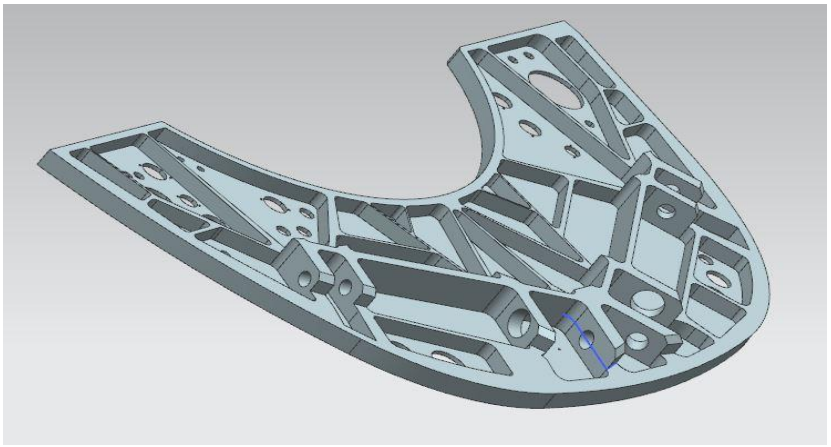

Figure 5: Isometric View of the Part FS 341.80

4.3 Determination of the Boundary Conditions and Forces Acting on the Part to be Analyzed

The boundary conditions to be applied to the part are in the sections where the part is mounted on the fuselage of the aircraft. The blue arrows in Figure 6 indicate the bolted connections at which the part is fixed.

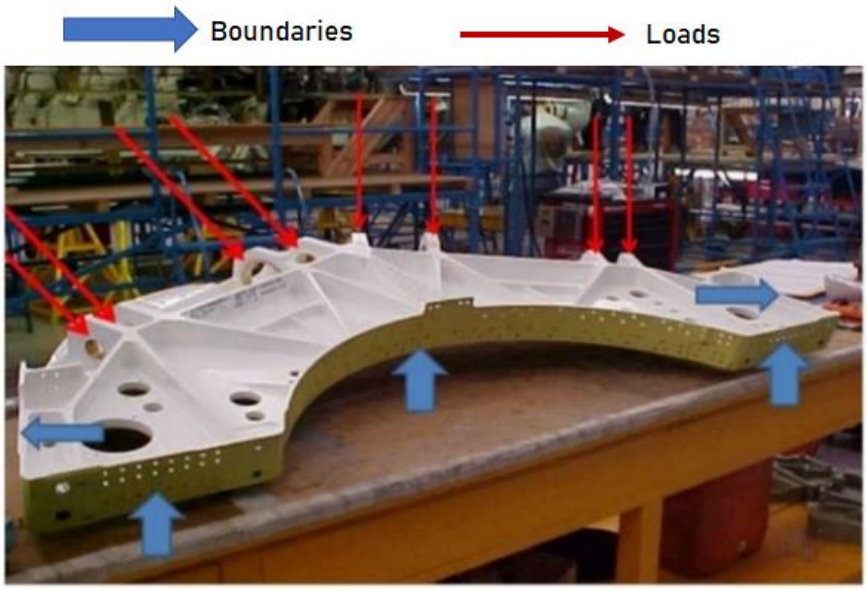

Figure 6: Forces Acting on Part FS 341.80

These connections are, from above to the upper part of the main landing gear, from the sides to the fuselage and from the curved central surface to the engine compartment. Loads acting during landing are shown in Figure 6 with red arrows. After the wheels hit the ground, the reaction force from the ground is transmitted to the part in the following order: wheels, aircraft beams, beam axles, holes on the part.

Thus the applied forces are distributed along the surfaces of the holes near the axles of the beams. These holes transfer all the loads, and the upper or lower inner surfaces of the holes are pressed depending on the compression or tension in the beams, respectively. Figure 7 shows the force acting on the upper inner surface of the hole when compression occurs in the relevant beams.

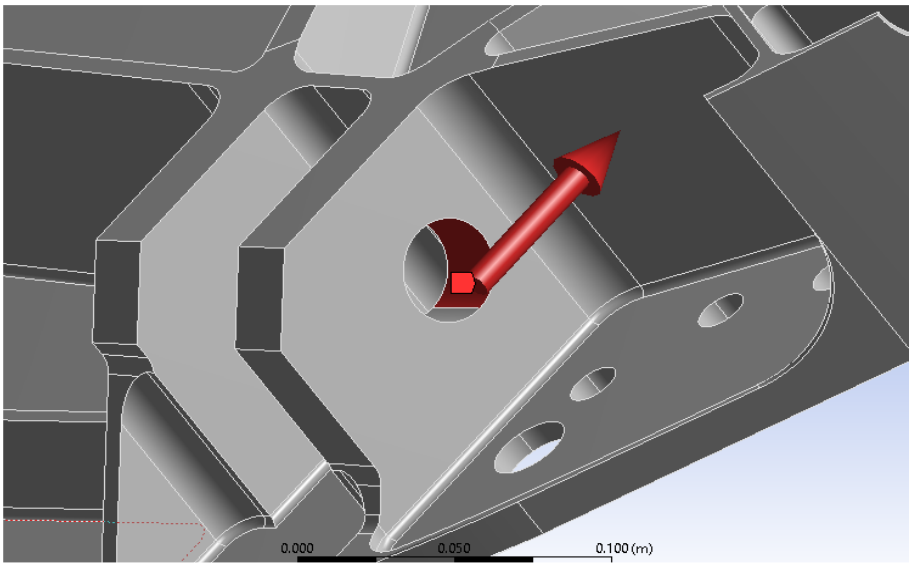

Figure 7: Force Acting on the Upper Inner Surface of the Hole

The force applied to the part through the wheels is calculated by Eq. (2) where mF16 denotes the mass of the aircraft, a_{F16} the acceleration and v_{land} the landing velocity in the direction of the ground reaction. Four different scenarios are defined in the next section and the mass of the aircraft is given in each related scenario.

$$F = m_{F16}.a_{F16} = m_{F16}\frac{v_{land}}{\Delta t} \quad (2)$$

Since the landing is very sudden in the form of an impact, the Δt value was accepted as 0.1 seconds. It is stated in the literature (Kesarwani, 2017) that the maximum landing speed of the F-16 for a safe landing is 160 knots, almost 82.31 m/s or more specifically 296.32 km/h when converted to SI units. The ideal angle of attack to land the F-16 is in the range of 11°<AoA<15° (Ramprasadh et al., 2018). Thus we assumed that Angle of Attack (AoA)=13°.

Figure 8: F-16 Landing
(www.savturk.com)

For a landing F-16, as seen in Figure 8, the velocity component in the direction of ground reaction at the moment the wheels touch the ground is calculated as follows, according to Figure 9:

$$v_{land} = v \sin AoA \tag{3}$$

Here, v is the speed of the aircraft in its direction of motion.

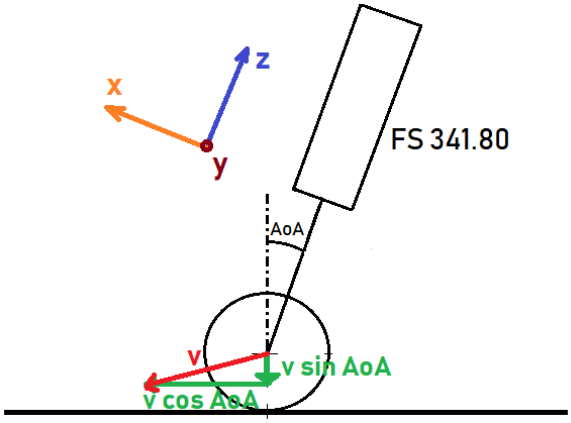

Figure 9: Diagram of velocity vectors acting on the wheel during landing

We calculate the mass of F-16 as:

$$m_{F16} = m_{mt} - m_{cmin} - m_{fuel} = 19200 - 4500 - 1000 = 13700 \text{ kg} \tag{4}$$

where, m_{mt} is the maximum take-off mass, m_{cmin} is the minimum ordnance mass at landing, and m_{fuel} is the minimum fuel mass consumed during the flight. Accordingly, the minimum safe mass of the aircraft on landing was assumed as 13700 kg.

In Figure 10, arrow number 1 is the shock absorber support, arrows number 2 and 3 are the pull supports. The main function of the shock absorber is to absorb and dissipate the impact kinetic energy until the acceleration applied to the body is reduced to an acceptable level. This assembly is a two-stage air-oil type shock support that produces a stepped air spring. Its fully extended length is 93.59 cm. The shock support is directly connected to the underside of the traction support and the track assembly at the rear end of the main gear case.

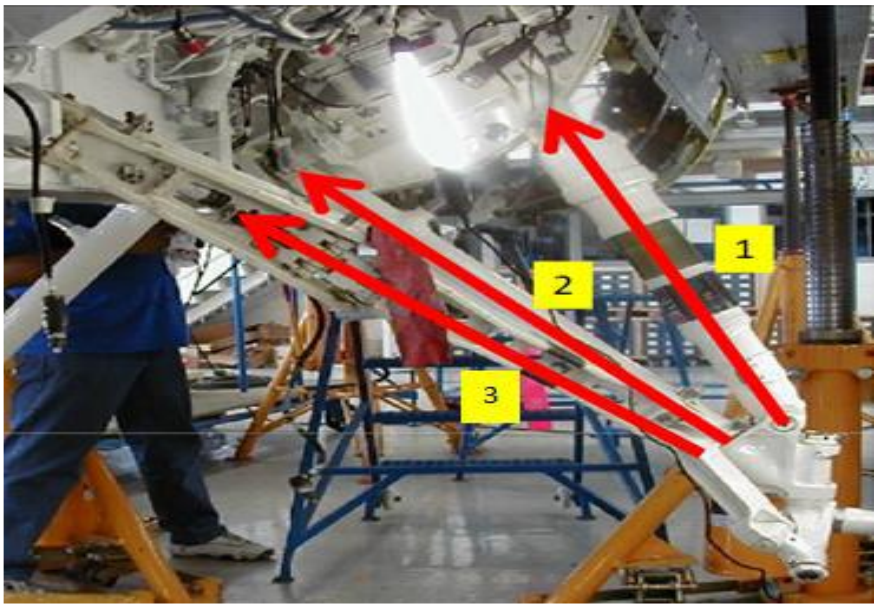

Figure 10: Shock and Pull Supports

Figure 11 shows the fixed boundaries in Ansys Workbench. Figure 12 shows the applied forces in Ansys Workbench.

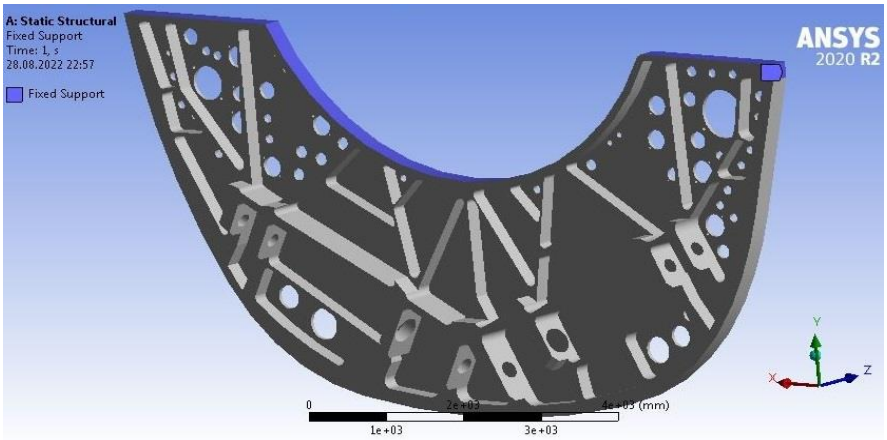

Figure 11: FS 341.80 Fixed Boundaries

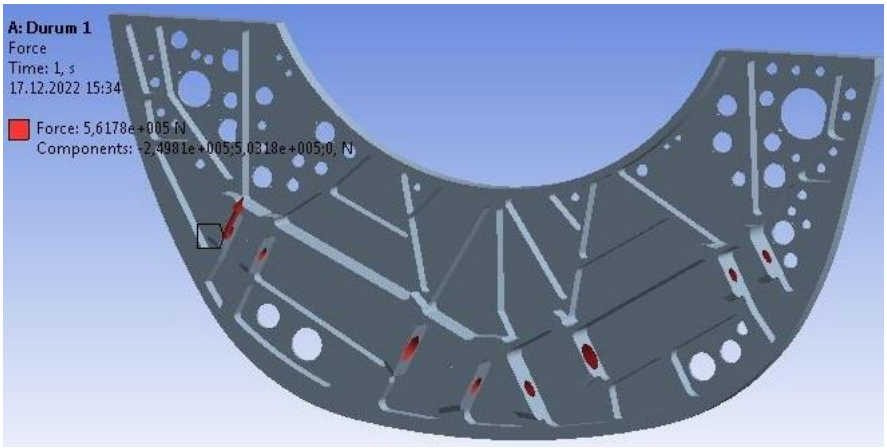

Figure 12: Forces Applied on FS 341.80

4.4 Four Different Scenarios Considered in the Analysis

For equivalent static analysis, four different scenarios were defined in which the landing mass and velocity of the aircraft varied.

Scenario 1: It's a typical F-16 landing. It is assumed that the aircraft took off with ordnance and returned by completing its mission, by sending the ordnance to the target. Landing mass: 13700 kg, landing speed: 160 knots (296.32 km/h). It is also assumed that the aircraft lands on two wheels in the ideal landing condition.

Scenario 2: It was assumed that the plane took off and had to make an emergency landing due to a malfunction that was detected in a very short time. In this case, its mass is taken to be approximately equal to the mass of the moment of take-off, that is, approximately 18750 kg. The landing speed is again 160 knots (296.32 km/h). Normally, in these situations, a significant percent of the fuel is deliberately discharged to reduce the mass of the aircraft during landing, but we neglected this discharge to stay on the safety side.

Scenario 3: The aircraft took off, completed its normal flight, and landed with the mass in Scenario 1. However, its speed at ground contact is 100 km/h (approx. 33%) higher than its normal landing speed; that is 396.32 km/h.

Scenario 4: Finally, it was assumed that the landing was not “perfect”, that is, the aircraft landed on one wheel of the main landing gear, not two wheels, at the first moment. In other words, it is assumed that the right wheel touches the ground at the first landing and the left wheel has not yet touched the ground. So the holes on the right side of part FS 34.180 will be forced twice of Scenario 1.

The four scenarios mentioned above are summarized in Table 2, and the forces acting on the holes of the part in each scenario are given in Table 3. The minus sign indicates compression.

Table 2: Four Different Landing Scenarios

Scenario #	Landing Mass	Landing velocity (km/h)	Gear contact single/double
1	13 700	296.32	double
2	18 750	296.32	double
3	13 700	396.32	double
4	13 700	296.32	single

Table 3: Forces on the Holes of the Part FS 34.180

Scenario #	Compressive force on the holes [kN]	Tensile force on the holes [kN]
1	– 1277.50	561.78
2	– 1748.40	768.85
3	– 1713.81	754.89
4	– 2555.50	1123.56

5. ANALYSIS

In the equivalent static analysis, it is aimed to calculate the equivalent stress, equivalent total strain, maximum shear stress and total deformation values that the part is exposed to due to the forces acting on the main landing gear wheels when they hit the ground.

5.1 Convergence Analysis

In order to ensure that the element size of the mesh is sufficient, a convergence analysis is performed. The results of the analysis are shown in Table 4. Finally, 20mm mesh element size of was selected at the 6th trial.

Table 4: Convergence Analysis

Trial	Mesh size (mm)	Number of nodes	Number of Elements	Equivalent stress (MPa)
1	30	481 035	264 566	57.821
2	28	562 589	311 947	54.167
3	26	642 423	358 281	55.423
4	24	778 136	438 998	54.696
5	22	929 569	527 475	57.878
6	20	1 077 259	614 274	60.525

The meshed view of the part is shown in Figure 13. There are 1 077 259 nodes and 614 274 Solid elements.

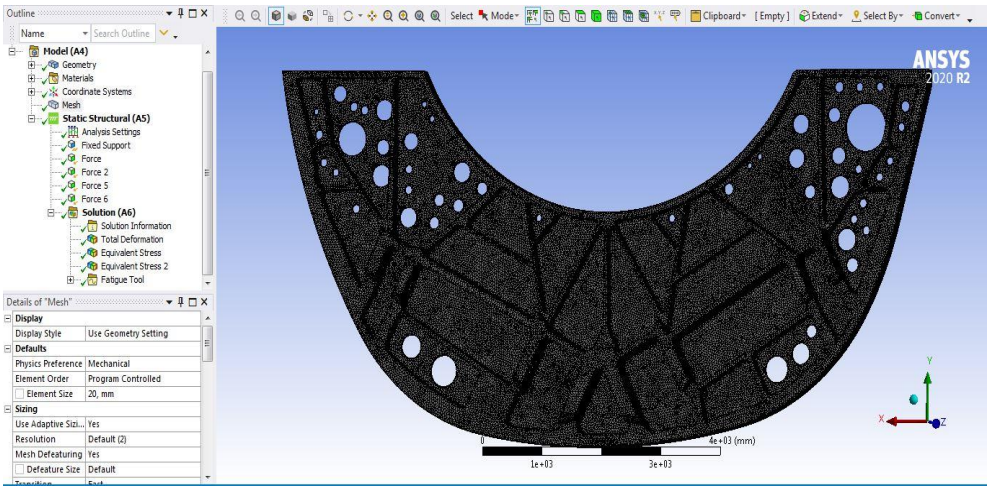

Figure 13: FS 341.80 Ansys Workbench mesh view (mesh size 2 mm)

5.2 Strength Analysis of Aluminum Alloy Part

The analysis of the existing part made of aluminum alloy was carried out for the 4 scenarios specified in Section 3.4. The equivalent stress and total deformation graphs for the most critical Scenario 4 are shown in Figures 14 and 15, respectively.

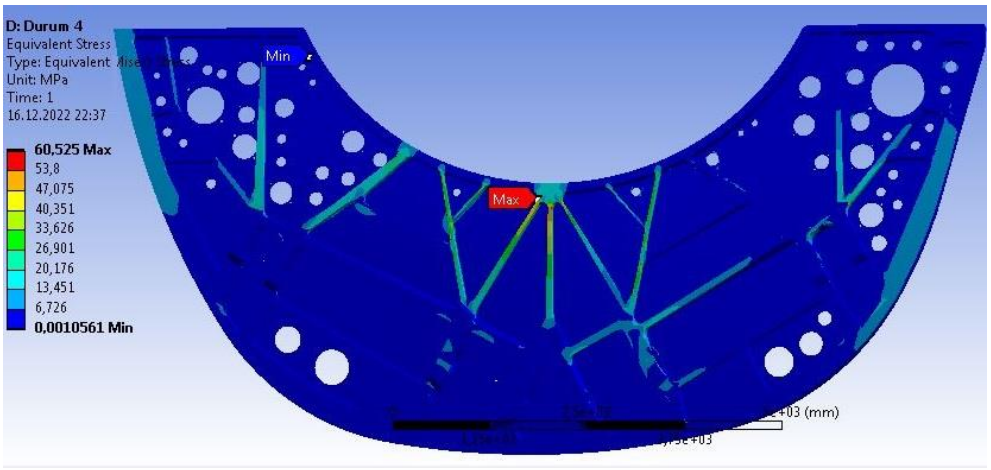

Figure 14: Aluminum alloy part equivalent stress graph for Scenario 4

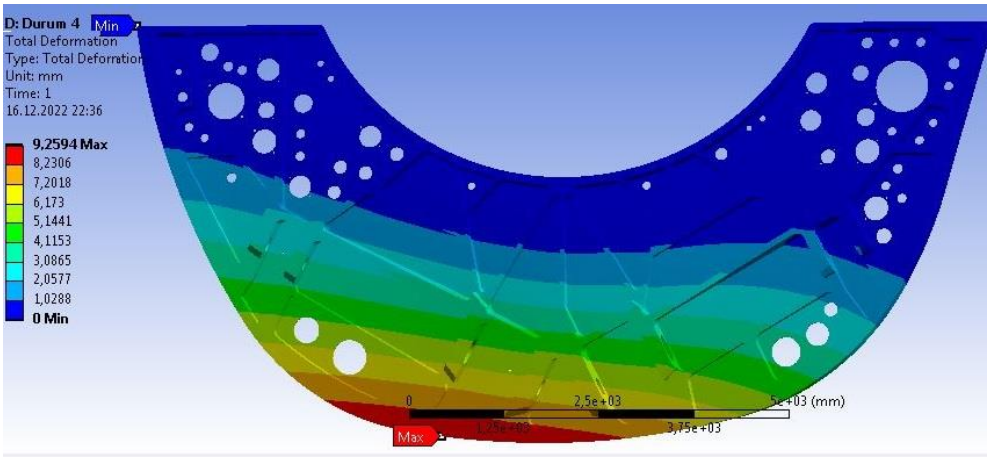

Figure 15: Aluminum alloy part total deformation graph for Scenario 4

5.3 Strength Analysis of CFRP Composite Part

The analysis of the part made of CFRP composite material was carried out for the 4 scenarios specified in Section 3.4. The equivalent stress, equivalent total strain, maximum shear stress and total deformation graphs for the most critical Scenario 4 are shown in Figures 16-19, respectively.

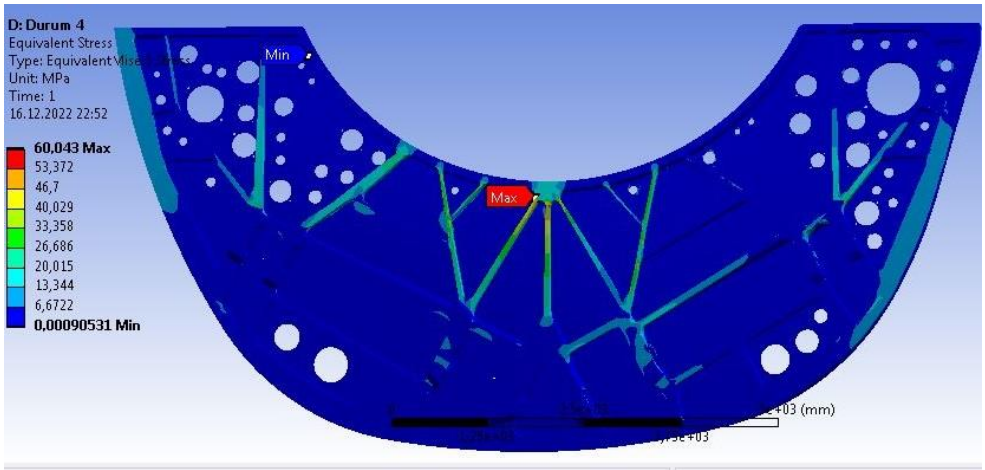

Figure 16: CFRP composite part equivalent stress graph for Scenario 4

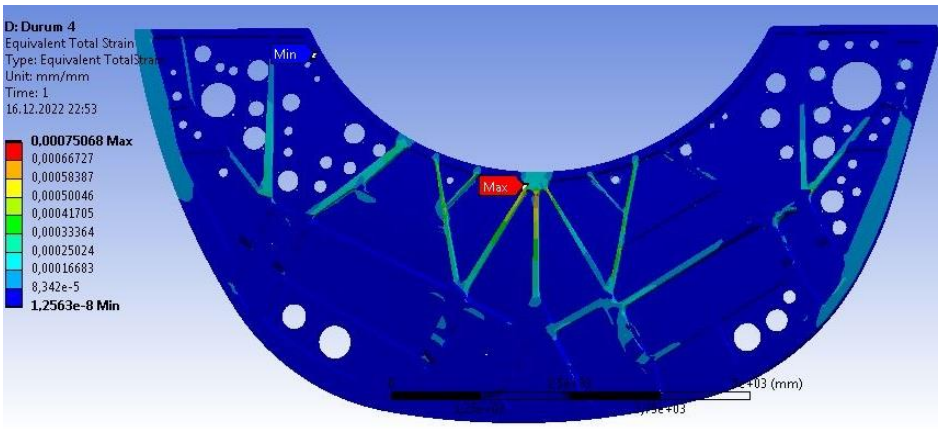

Figure 17: CFRP composite part equivalent total strain graph for Scenario 4

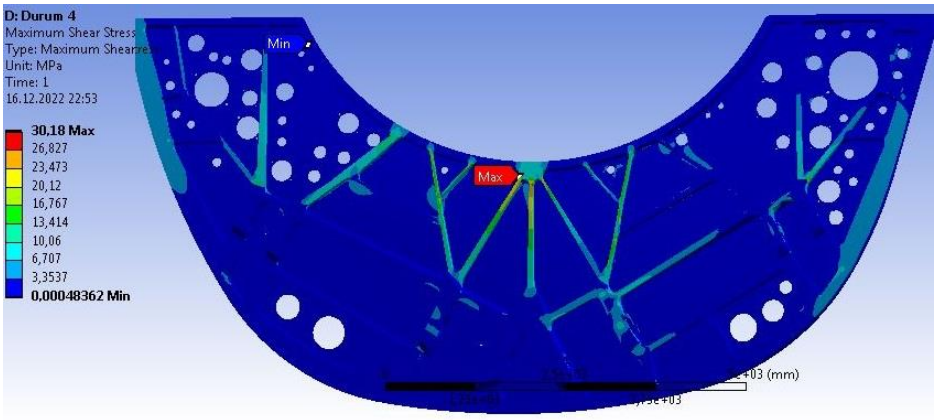

Figure 18: CFRP composite part maximum shear stress graph for Scenario 4

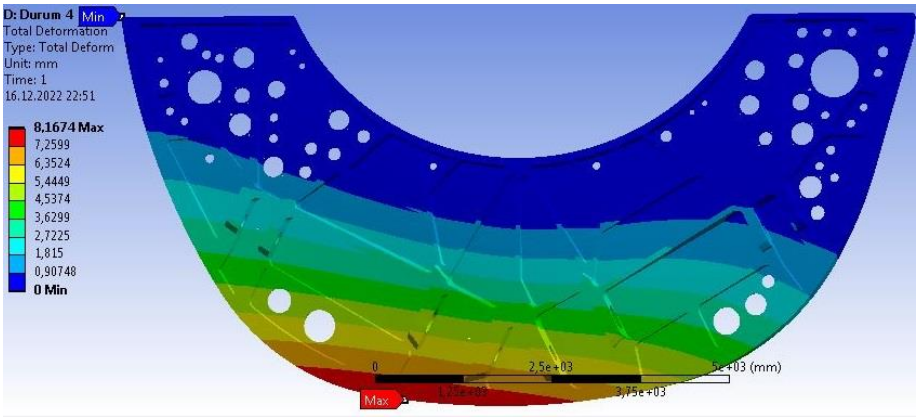

Figure 19: CFRP composite part total deformation graph for Scenario 4

5.4 Comparison of Analysis Results

Table 5 shows the equivalent (von Mises) stress values in FS 34.180 structural part for aluminum alloy and CFRP composite material. There is a very slight decrease of less than 0.8% in CFRP composite.

Table 5: Equivalent Stress Values (MPa) in FS 34.180 Structural Part

Case #	Aluminum	CFRP Composite	% Change
1	30.263	30.021	– 0.7997

2	41.418	41.088	– 0.7968
3	40.545	40.222	– 0.7966
4	60.525	60.043	– 0.7964

Table 6 shows the equivalent total strain values in FS 34.180 structural part for aluminum alloy and CFRP composite material. There is a decrease of about 12% in CFRP composite.

Table 6: Equivalent Total Strain Values in FS 34.180 Structural Part

Case #	Aluminum	CFRP Composite	% Change
1	0.00042319	0.00037260	– 11.9544
2	0.00050099	0.00044112	– 11.9503
3	0.00056698	0.00049921	– 11.9528
4	0.00084621	0.00075068	– 11.2892

Table 7 shows the maximum shear stress values in FS 34.180 structural part for aluminum alloy and CFRP composite material. There is a very slight decrease of about 0.7% in CFRP composite.

Table 7: Maximum Shear Stress Values (MPa) in FS 34.180 Structural Part

Case #	Aluminum	CFRP Composite	% Change
1	0.00042319	0.00037260	– 11.9544
2	0.00050099	0.00044112	– 11.9503
3	0.00056698	0.00049921	– 11.9528
4	0.00084621	0.00075068	– 11.2892

Table 8 shows the total deformation values in FS 34.180 structural part for aluminum alloy and CFRP composite material. There is a decrease of about 11.8% in CFRP composite.

Table 8: Total Deformation Values (mm) in FS 34.180 Structural Part

Case #	Aluminum	CFRP Composite	% Change
1	4.6297	4.0837	– 11.7934
2	6.3363	5.5890	– 11.7939
3	6.2028	5.4712	– 11.7947
4	9.2594	8.1674	– 11.7934

In Table 9, it is seen that the weight of the part is reduced by 33.37% as a result of the use of CFRP composite material.

Table 9: Comparison of Masses (kg) of FS 34.180 Structural Part for Two Materials

Aluminum	CFRP Composite	% Change
31.17	20.77	33.37

6. CONCLUSION

The strength analysis of the existing aluminum alloy FS 341.80 structural part operated in the F-16 aircraft was made with Ansys Workbench. Another analysis was made for the CFRP composite with the

same technical dimensions. In both analyses, the loads were calculated according to four different scenarios, taking into account the situations that the aircraft may encounter during landing.

As a result of the analyses made according to the scenarios; the equivalent (von-Mises) stress value was reduced by about 0.8%, the equivalent total strain value by 12%, the maximum shear stress value by 0.7% and the total deformation value by 11.8%. The mass of the analyzed F-16 part was reduced from 31.17 kg to 20.77 kg when CFRP composite material with similar strength properties was used instead of aluminum alloy, thus the weight of the part was reduced by 33.37 percent.

This weight reduction is for a single part, and when this analysis is carried out for other structural parts, the total weight reduction will be much higher. Thus, the operational capability of the F-16 aircraft would be enhanced by increasing the amount of ordnance and fuel optimization, and our aircrafts will be used more effectively in the field.

In today's conditions, the production of composite materials that will provide these analysis results would be costly and difficult. However, due to the developing technology, the search for new materials, studies in the field of aviation, and the development of operational doctrines, more structural parts will be produced and used with composite materials.

REFERENCES

Adeniran, O., Cong, W., & Aremu, A. (2022). Material design factors in the additive manufacturing of Carbon Fiber Reinforced Plastic Composites: A state-of-the-art review. *Advances in Industrial & Manufacturing Engineering, 5*, 1-18. https://doi.org/10.1016/j.aime.2022.100100

Altuntaş, G., & Bostan, B. (2022). Metallurgical characterization of natural aging effects on pre-deformed Al 7075/T651 alloy during retrogression and re-aging heat treatment. *Kovove Materialy-Metallic Materials, 60(4),* 209-222. doi.org/10.31577/km.2022.4.209

Atique, Md S.A., Probha, N.N., & Nafi, A.S. (2014, Dec 26-27). Polymer composites: a blessing to modern aerospace engineering. International Conference on Mechanical, Industrial and Energy Engineering, Khulna, Bangladesh. ICMIEE-PI-1402870

Battelle Memorial Institute. (2023). *MMPDS Metallic materials properties development and standardization handbook.*

Cevik, M. (2009). Effects of fiber orientation on out-of-plane and in-plane natural frequencies of angle-ply laminated composite arches. *Journal of Reinforced Plastics and Composites, 28(1),* 59-71. https://doi.org/10.1177/0731684407083003

Crosby, F. (2015). *The Complete Guide to Fighters & Bombers of the World*. Lorenz Books. https://www.amazon.in/Complete-Guide-Fighters-Bombers-World/dp/1846810000

Deo, R.B., Starnes, J.H., & Holzwarth, R.C. (2003). *Low-Cost Composite Materials and Structures for Aircraft Applications*. https://api.semanticscholar.org/CorpusID:111092384

Diambu, A. N., & Çevik, M. (2022, May 20-21). Finite element vibrational analysis of a porous functionally graded plate. 6th International Students Science Congress, İzmir, Türkiye. https://doi.org//10.52460/issc.2022.041

Esen, Y., & Ülker, M. (2005). Optimization of materially non-linear multi storey spaces frames by ANSYS. *Doğu Anadolu Bölgesi Araştırmaları, 3(3),* 127-131. https://dergipark.org.tr/tr/pub/fudad/issue/47052/591656

Faizan, M., & Gangwar, S. (2021). Tensile behaviour of carbon fiber reinforced polymer composite using ANSYS 21. *Materials Today: Proceedings, 46(15),* 6519-6526. https://doi.org/10.1016/j.matpr.2021.03.724

Godara, S.S., Brenia, V., Soni, A.K., Shekhawat, R.S., & Saxena, K.K. (2022). Design & analysis of connecting rod using ANSYS software. *Materials Today: Proceedings, 56(4),* 1896-1903. https://doi.org/10.1016/j.matpr.2021.11.166

Gökçe, H. (2021). Investigation of drilling performance of Al 1050-H14 alloy with high ductility. *The Journal of Defense Sciences, 39,* 179-209. https://doi.org/10.17134/khosbd.913742

Göker, Ü.D., Yazıcı, M., Balcı, G., Köksal, Ö., & Şengelen, H.E. (2021). The statistical analysis of air crash investigations from 1918 to 2019. *The Journal of Defense Sciences, 2(40),* 1-32. https://doi.org/10.17134/khosbd.1000317

Guo, R., Li, C., Niu, Y., & Xian, G. (2022). The fatigue performances of carbon fiber reinforced polymer composites - A review. *Journal of Materials Research and Technology, 21,* 4773-4789. https://doi.org/10.1016/j.jmrt.2022.11.053

Han, H.K., Kim, H.S., & Sohn, S.Y. (2009). Sequential association rules for forecasting failure patterns of aircrafts in Korean airforce. *Expert Systems with Applications, 36(2-1),* 1129-1133. https://doi.org/10.1016/j.eswa.2007.10.012

Hassan, A.H.A., & Kurgan, N. (2019). Modeling and Buckling Analysis of Rectangular Plates in ANSYS. *International Journal of Engineering & Applied Sciences, 11(1),* 310-329. https://doi.org/10.24107/ijeas.531011

Holt, J.M., Mindlin, H., & Ho, C.Y. (1997). *Structural Alloys Handbook*. CINDAS.

Jung, C., Kang, Y., Song, H., Lee, M.G., Jeon, Y. (2022). Ultrasonic fatigue analysis of 3D-printed carbon fiber reinforced plastic. *Heliyon, 8,* e11671, 1-11. https://doi.org/10.1016/j.heliyon.2022.e11671

Kandaş, H., & Özdemir, O. (2022). Effects of bio-particles on mechanical and quasi-static punch shear behaviors of glass/epoxy composites. *Scientific Research Communications, 2(2),* 1-9. https://doi.org/10.52460/src.2022.010

Karslı, M., Sert, Y., & Küçükömeroğlu, T. (2020). Development of polymer composite material for gun frames. *The Journal of Defense Sciences,* 38, 131-157. https://dergipark.org.tr/en/pub/khosbd/issue/57672/814023

Kesarwani S. (2017). Polymer Composites in Aviation Sector: A Brief Review Article. *Int. Journal of Engineering Research & Technology, 6(6),* 518-525. https://www.ijert.org/polymer-composites-in-aviation-sector

Logan, D.L. (2016). *A First Course in the Finite Element Method*. Thomson. ISBN: 0-534-55298-6

Mangalgiri, P.D. (1999). Composite materials for aerospace applications. *Bulletin of Materials Science, 22(3),* 657-664. https://doi.org/10.1007/BF02749982

Megson, T. H. G. (2018). *Introduction to Aircraft Structural Analysis* (3rd Edition). Butterworth-Heinemann. ISBN: 9780081020760

Mrazova, M. (2013). Advanced composite materials of the future in aerospace industry. *INCAS Bulletin, 5(3),* 139-150. https://doi.org/10.13111/2066-8201.2013.5.3.14

Mouritz, A.P. (2012). Aluminium alloys for aircraft structures, *Introduction to Aerospace Materials*, Woodhead Publishing, 173-201. https://doi.org/10.1533/9780857095152.173

Müftü, S. (2022). *Finite Element Method, Physics & Solution Methods*. Academic Press. https://doi.org/10.1016/C2019-0-02993-7

Nayak, N. V. (2014). *Composite Materials in Aerospace Applications*. CorpusID: 8443806.

Özer, A. (2016). The microstructures and mechanical properties of Al-15Si-2.5Cu-0.5Mg/(wt%)B_4C composites produced through hot pressing technique and subjected to hot extrusion. *Materials Chemistry and Physics, 183,* 288-296. https://doi.org/10.1016/j.matchemphys.2016.08.029

Özer, M., Aydoğan, S.İ., Çinici, H., & Özer, A. (2022). Effects of sintering techniques and parameters on microstructure and mechanical properties of Al-15Si-2,5Cu-0.5Mg compacts and Al-15Si-2,5Cu-0.5Mg/B_4C composites. *Materials Today Communications, 30,* 103192. https://doi.org/10.1016/j.mtcomm.2022.103192

Pan, R., Wang, P., Jiang, S., Yang, W., Wu, P., Qiao, J., Chen, G., & Wu, G. (2023). Effect of lattice constants and precipitates on the dimensional stability of rolled 2024Al during isothermal aging. *Materials, 16(4),* 1440. https://doi.org/10.3390/ma16041440

Ramprasadh, C., Prem, S., Sankaralingam, L., Deshpande, P., Dodamani, R., & Suraj, C.S. (2018). A simple method for estimation of angle of attack. *IFAC-PapersOnLine, 51(1),* 353-358. https://doi.org/10.1016/j.ifacol.2018.05.048

Savran, M., Yılmaz, M., Öncül, M., & Sever, M. (2022). Manufacturing and modeling of polypropylene-based hybrid composites by using multiple-nonlinear regression analysis. *Scientific Research Communications, 2(1),* 1-15. https://doi.org/10.52460/src.2022.002

Silori, P., Shaikh, A., Kumar, K.C., Tandon, T. (2015). Finite element analysis of traction gear using ANSYS. *Materials Today: Procs.,* 2, 2236-2245. https://doi.org/10.1016/j.matpr.2015.07.243

Starke, E.A., & Staley, J.T. (1996). Application of modern aluminum alloys to aircraft. *Progress in Aerospace Sciences, 32(2-3),* 131-172. https://doi.org/10.1016/0376-0421(95)00004-6

Stolarski, T., Nakasone, Y., Yoshimoto, S. (2018). *Engineering Analysis with ANSYS Software*. Butterworth-Heinemann. https://doi.org/10.1016/C2016-0-01966-6

Sunar, Ö., & Çevik, M. (2015). Fatigue analysis of single leaf springs with finite element method. *Celal Bayar University Journal of Science, 11(1),* 1-6. https://doi.org/10.18466/cbufbe.34361

Tunca, E., & Kafalı, H. (2021). Compression and three-point bending analyzes of aerospace sandwich composites produced with polymeric core materials using ANSYS. *European Journal of Science & Technology, 31(1),* 553-561. https://doi.org/10.31590/ejosat.1012658